

A COMPARATIVE STUDY OF UNET VARIANTS FOR LOW-GRADE GLIOMA SEGMENTATION IN MAGNETIC RESONANCE IMAGING

Yasin GÜZEL¹ 

Zafer AYDIN² 

¹Süleyman Demirel University, Faculty of Education, Isparta

²Abdullah Gül University, Electrical and Computer Engineering, Kayseri

Article Info

Received: 15 April 2025

Accepted: 14 May 2025

Keywords

Brain tumor,
Deep learning,
Health,
Low grade glioma,
Segmentation

ABSTRACT

Brain tumors originating from glial cells are pathological entities that significantly impact quality of life and are classified based on their malignancy into low-grade gliomas (LGGs) and high-grade gliomas (HGGs). While the more aggressive HGGs have been extensively studied, LGGs are of critical importance for early diagnosis due to their potential progression to HGGs if left untreated. This has driven researchers to develop methods for the rapid and consistent diagnosis of LGGs. In this study, three models—UNet, Transformer UNet, and Super Vision UNet—were comparatively evaluated for the automatic segmentation of LGGs using magnetic resonance imaging (MRI) data. Multimodal MRI scans from 110 patients, retrieved from The Cancer Imaging Archive (TCIA), were used to train the models. Performance was evaluated using Dice Coefficient, Tversky Index, and Intersection over Union (IoU) metrics. The Super Vision UNet achieves the highest Dice (0.9115) and Tversky (0.9154) scores, while the Transformer UNet attains the highest IoU (0.8789). Both advanced models demonstrate superior segmentation performance with lower loss values compared to the conventional UNet. Visual outputs indicate that the modern architectures delineate tumor contours with greater precision. These results highlight the effectiveness and reliability of contemporary UNet-based and Transformer-based architectures in segmenting complex tumor structures such as LGGs. Integrating these models into clinical decision support systems holds promise for enhancing the speed and accuracy of the diagnostic process.

INTRODUCTION

Brain tumors are abnormal growths that can seriously affect the central nervous system and significantly reduce a patient's quality of life (Ostrom et al., 2014). These tumors are typically categorized into two main types: low-grade gliomas (LGGs) and high-grade gliomas (HGGs). Gliomas, which arise from glial cells, constitute the most frequently occurring brain tumors. Based on their growth rate and level of malignancy, gliomas are divided into different grades. According to the World Health Organization (WHO) classification, they are categorized into four grades, from Grade I to Grade IV (Louis et al., 2016).

Among them, glioblastomas (Grade IV), which are a type of HGG, are the most aggressive and have the lowest survival rates (Sanai & Berger, 2008). Because of this, most

Yasin GÜZEL ✉, yasinguzel@sdu.edu.tr

Süleyman Demirel University, Faculty of Education, Isparta

research and funding have focused on HGGs, while LGGs have received less attention (Van Dijken, Van Laar, Holtman, & Van Der Hoorn, 2017). However, LGGs can slowly grow and spread into surrounding brain tissue. If not treated early, they may develop into HGGs, which makes them more dangerous over time (Ostrom et al., 2014). This highlights the need for more research on the diagnosis and treatment of LGGs.

Features such as the tumor's size, shape, grade, and location are very important for deciding on the right treatment (Ostrom et al., 2014). One of the first steps in diagnosing a brain tumor is medical imaging, especially Magnetic Resonance Imaging (MRI) (Van Dijken et al., 2017). MRI is a non-invasive method that provides detailed images of the brain and is widely used to detect brain tumors (Ghadimi et al., 2025).

A critical part of analyzing MRI scans is the segmentation process. Segmentation means identifying and outlining the tumor area in the image. This helps doctors understand where the tumor is and how big it is, which is useful for diagnosis and treatment planning (Verma, Shivhare, Singh, Kumar, & Nayyar, 2024). Although manual segmentation by experts is still considered the most reliable method, it takes a lot of time, requires expertise, and may vary between observers. To address these challenges, researchers have increasingly focused on developing automated segmentation systems.

In recent years, deep learning methods—especially models based on UNet and transformer architectures—have demonstrated remarkable performance in medical image analysis and segmentation. These technologies allow for fast and accurate tumor detection. In this study, we test the performance of UNet and its variants in segmenting LGGs from brain MRI images.

The remainder of this paper is structured as follows. The next section presents a review of related work in the field of brain tumor segmentation using deep learning. This is followed by a detailed description of the materials and methods used, including the datasets, preprocessing steps, model architectures, and evaluation metrics. Subsequently, the experimental results and their discussion are provided, highlighting the models' performance across the test dataset. Finally, the paper concludes with a summary of the findings and potential directions for future research.

Related Works

This section presents previous studies focused on the segmentation of low-grade gliomas (LGGs). Naser and Deen (2020) developed a deep learning-based approach for segmenting brain tumors and grading LGGs using magnetic resonance imaging (MRI). In their study, a

UNet-based convolutional neural network (CNN) was used for tumor segmentation, while a VGG16-based transfer learning model was employed for tumor grading. The segmentation model was trained on a dataset consisting of T1-precontrast, FLAIR, and T1-postcontrast MRI scans from 110 patients, achieving a Dice Similarity Coefficient (DSC) of 84%.

Lefkovits, Lefkovits, and Szilágyi (2022) developed a CNN-based system for the segmentation of both high-grade (HGG) and low-grade gliomas (LGG) using the Amazon SageMaker platform. Six different CNN models were trained on BraTS 2017–2020 datasets, and the best-performing model was selected through hyperparameter optimization. Furthermore, an ensemble model was created based on the weighted average of these models to improve the accuracy of tumor boundary detection. The results were compared with the Dice scores from the BraTS 2020 challenge, and the proposed method ranked within the top 25%.

Shomirov, Zhang, and Billah (2022) addressed the class imbalance problem in tumor segmentation by introducing a 3D UNet model with a Weighted Focal Loss (WFL) function. Designed for both HGG and LGG segmentation, the model was tested on the BraTS 2019 and 2020 datasets. It demonstrated high accuracy in segmenting tumor core (TC), whole tumor (WT), and enhancing tumor (ET) regions.

BabaAhmadi and FallahPour (2023) conducted a comparative study on three models for LGG segmentation: DeepLabV3+, UNet, and a novel Transformer-based approach. Their findings showed that the MobileNetV3-based DeepLabV3+ model achieved the best overall performance. However, the Transformer-based model demonstrated superior segmentation accuracy, memory efficiency, and adaptability to different image sizes. Additionally, transfer learning techniques were applied to further improve the models' performance.

Similarly, Wan et al. (2023) proposed a segmentation model based on DeepLabV3+ and RegNet, which incorporated not only MRI scans but also patients' genetic data and clinical information for a more comprehensive analysis. The model included a novel loss function called outlier-region loss, designed to reduce the influence of small, misclassified areas. Experiments on the Lower-Grade Glioma (LGG) Segmentation dataset yielded a Dice score of 94.36% and an Intersection over Union (IoU) score of 91.83%, outperforming several existing methods.

Dattangire, Biradar, and Joon (2024) proposed a UNet-based AI-assisted model for LGG segmentation. Aiming to address the challenges of manual segmentation caused by the heterogeneous nature of tumors, their model was designed to support radiologists through automated segmentation. Trained on the BraTS dataset, the model was evaluated using accuracy, Dice score, and IoU metrics, and the results indicated that it could be effectively integrated into clinical decision support systems.

Bentaher et al. (2025) present R2A-UNET, a deep learning model for accurate glioma segmentation in medical images. By integrating residual blocks with channel and spatial attention mechanisms (NCA and NSA), the model enhances feature extraction and focuses on relevant regions. It achieved high DSC and IoU scores on both the LGG and BraTS 2018 datasets, and demonstrated strong cross-dataset generalizability. Grad-CAM visualizations and Wilcoxon ranksum tests further validated its clinical potential.

MATERIAL AND METHOD

The Dataset

The dataset utilized in this research was sourced from The Cancer Imaging Archive (TCIA) and consists of clinical and imaging data from 110 patients diagnosed with low-grade gliomas (LGGs) (Pedano et al., 2016). The patients were collected from five different medical institutions. Among them, 50 were classified as Grade II, 58 as Grade III, while 2 patients had unknown tumor grades and 1 had an unspecified tumor subtype. The tumors were categorized into three subtypes: Astrocytoma, Oligoastrocytoma, and Oligodendroglioma. The distribution of these tumor types is shown in Table 1.

Preoperative imaging data include three MRI sequences: non-contrast-enhanced T1-weighted (T1), FLAIR, and contrast-enhanced T1-weighted (T1CE) images. Each patient has between 20 and 88 slices, each with a resolution of 256×256 pixels. A total of 3,929 images were used, comprising 1,373 images containing tumors and 2,556 without visible tumor regions. Figure 1 presents sample slices from five patients in the dataset. These include the non-contrast T1, FLAIR, and contrast-enhanced T1 sequences. To aid interpretation, Figure 1 also shows a merged visualization of the three modalities, a FLAIR image with a hot colormap for improved contrast, and the tumor region overlaid on the merged image.

Segmentation masks were manually annotated by Buda et al. (2019) based on FLAIR images. These annotations are publicly available in TIF format along with the corresponding MRI scans. Each sample in the dataset consists of a three-channel image, where the channels represent the non-contrast T1, FLAIR, and contrast-enhanced T1 sequences. In cases where imaging data were incomplete (six patients missing T1 and nine missing T1CE images), the missing channels were filled using available FLAIR scans to ensure data consistency.

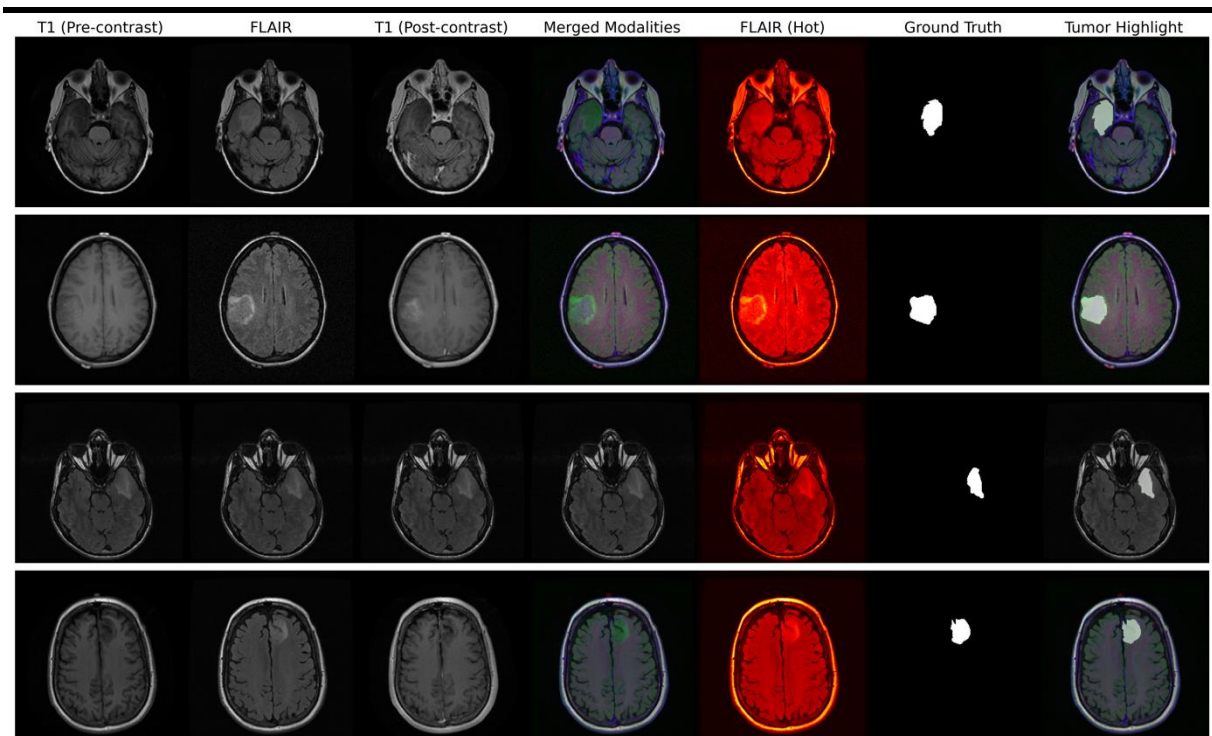


Figure 1. Visualization of multimodal brain MRI scans from five patients diagnosed with low-grade glioma. Each row represents a different patient. The columns show: (1) T1-weighted (pre-contrast), (2) FLAIR, (3) T1-weighted (post-contrast), (4) a merged visualization of the three modalities, (5) FLAIR with a hot colormap for enhanced contrast, (6) the ground truth tumor mask, and (7) the tumor region overlaid on the merged image.

Table 1. Distribution of Tumor Grades and Subtypes in Low-Grade Glioma (LGG) Cohort

	Grade II	Grade III	Unknown
Tumor sub-types			
Astrocytoma	8	26	-
Oligoastrocytoma	14	14	1
Oligodendroglioma	28	18	-
Unknown	-	-	1
Total	50	58	2

To minimize bias and enhance the reliability of model evaluation, the dataset was randomly partitioned at the patient level into three distinct subsets: training, validation, and testing. Specifically, 70% of the patients (77 patients) were assigned to the training set, 15% (16 patients) to the validation set, and 15% (17 patients) to the test set. As a result, the training set contains 2,738 images, the validation set includes 579 images, and the test set comprises 612 images. Dividing the dataset by patient ensures that images from the same individual are not split across different subsets, thereby allowing a more accurate assessment of the model's generalization performance. Prior to model training, min-max normalization was applied to all images to scale pixel intensity values to the [0, 1] range. This preprocessing step helps improve numerical stability during training and ensures that the input data is standardized across all subsets.

The Deep Learning Models Used

In this study, three state-of-the-art deep learning models commonly employed for semantic segmentation tasks were utilized: UNet (Ronneberger, Fischer, & Brox, 2015), Supervision UNet (Le'Clerc Arrastia et al., 2021), and Transformer UNet (Petit et al., 2021). The models were developed using Python (v3.10) and the TensorFlow framework (v2.11) for deep learning. Among these, the architecture of the Supervision UNet model, which achieved the lowest loss value during training, is illustrated in Figure 2.

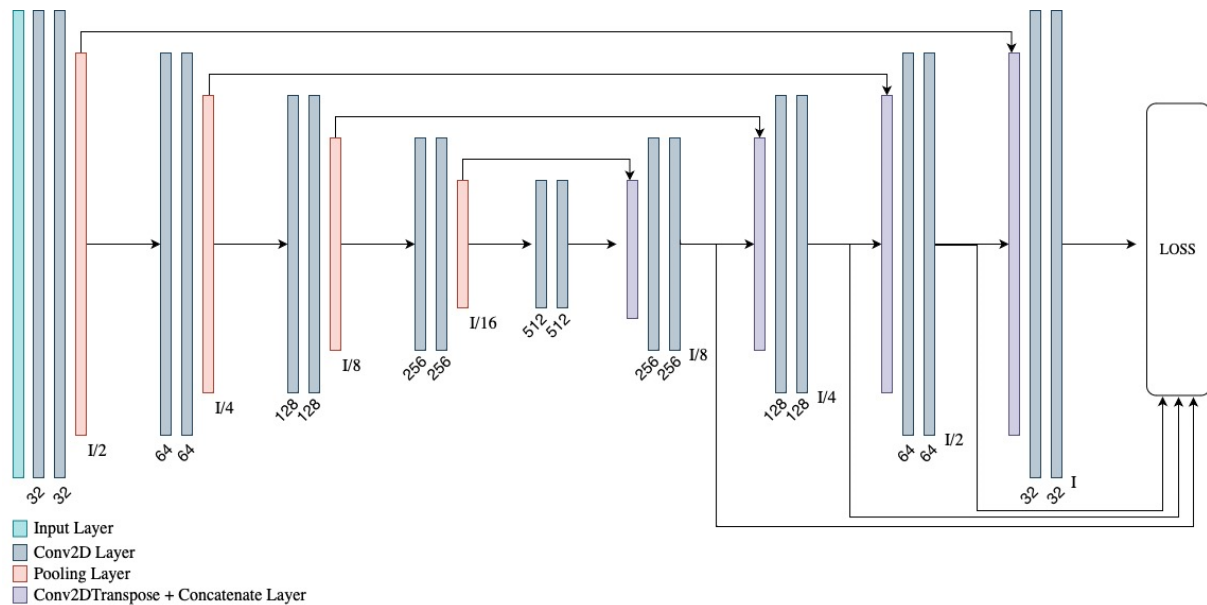


Figure 2. The architecture of Super Vision UNet

To effectively train the models, several data augmentation techniques were applied during preprocessing. Specifically, standard augmentation methods such as random rotations and horizontal flips were utilized. These data augmentation techniques were applied exclusively to the training dataset in order to increase data diversity, improve model performance, prevent overfitting, and enhance generalization ability. In the context of segmentation tasks, all transformations were synchronously applied to both the input images and their corresponding ground truth masks to preserve spatial consistency. These augmentations were implemented on-the-fly during training, meaning that each epoch was exposed to slightly different versions of the original training images. Although the total number of stored images remained unchanged, the effective size and variability of the dataset were significantly increased through dynamic augmentation. In addition, hyperparameter optimization was carried out to fine-tune critical parameters that are not learned during training but significantly influence performance, such as learning rate and batch size. A grid search strategy was adopted for hyperparameter optimization. Specifically, batch sizes of 2, 4, and 8, loss functions including Binary Cross

Entropy (BCE) and Dice Loss (Milletari, Navab, & Ahmadi, 2016), and learning rates of 1×10^{-2} , 1×10^{-3} and 1×10^{-4} were tested. The optimal combinations were selected based on the models' performance on the validation set. In all models, the number of training epochs was set to 150, and an early stopping mechanism with a patience value of 15 was employed. This configuration was designed to ensure a balanced and effective training process, maximizing both model accuracy and generalization capacity.

Evaluation Metrics

To assess the performance of the segmentation models proposed in this research, three widely used metrics from the literature were employed: the Tversky Index (Tversky, 1977), Intersection over Union (IoU) (also known as the Jaccard Index) (Jaccard, 1912), and the Dice Coefficient (Milletari et al., 2016).

The Tversky Index is a similarity measure between the predicted and ground truth regions, commonly used in segmentation tasks. It can be considered a generalization of both the Dice and Jaccard indices. What makes the Tversky Index particularly valuable is its flexibility in handling imbalanced class distributions. By introducing the parameters α and β , it allows different weights to be assigned to false positives (FP) and false negatives (FN), making it especially effective in medical imaging applications where class imbalance is a common challenge. The Tversky Index is defined mathematically as shown in Equation (1):

$$Tversky\ Index = \frac{TP}{TP + \alpha \cdot FP + \beta \cdot FN} \quad (1)$$

where TP (True Positives) refers to pixels correctly predicted as part of the tumor, FP (False Positives) are pixels incorrectly predicted as tumor, and FN (False Negatives) are actual tumor pixels missed by the model. α and β are hyperparameters that balance the penalties for FP and FN, respectively.

The Dice Coefficient, shown in Equation (2), offers a harmonic balance between precision and recall, providing a comprehensive evaluation of segmentation quality. It is especially effective when measuring overlap between predicted and actual tumor regions.

$$Dice\ Coeff = \frac{2 \cdot TP}{2 \cdot TP + FP + FN} \quad (2)$$

The Intersection over Union (IoU) metric, which directly measures segmentation accuracy, quantifies the overlap between the predicted region and the ground truth region. It is calculated using Equation (3):

$$IoU = \frac{TP}{TP + FP + FN} \quad (3)$$

By combining these three metrics, the segmentation performance of each model can be assessed comprehensively, considering not only overall accuracy but also sensitivity to class imbalance and boundary precision.

RESULTS AND DISCUSSION

The test set performance of the models is presented in Table 2, and the hyperparameters that contributed to these results are shown in Table 3. Additionally, example segmentation outputs for visual comparison are provided in Figure 3. As indicated in Table 2, segmentation performance was significantly improved by the Transformer UNet and Super Vision UNet, relative to the baseline UNet model across all major evaluation metrics. These models achieved lower loss values while improving the Dice Coefficient, Tversky Index, and IoU scores.

Specifically, Super Vision UNet achieved the highest scores in Dice Coefficient (0.9115) and Tversky Index (0.9154), whereas Transformer UNet reached the best performance in IoU (0.8789). These metrics are key indicators of segmentation quality, as they reflect how accurately the model delineates tumor boundaries and how strongly the predicted tumor region overlaps with the ground truth.

Table 2. Performance of Deep Learning Models on the Test Dataset

Models	Loss	Tversky Index	Dice Coeff	IoU
Transformer UNet	0.1364	0.9091	0.9073	0.8789
Super Vision UNet	0.0934	0.9154	0.9115	0.8777
UNet	0.1346	0.8663	0.8654	0.8341

Table 3. Optimally Tuned Hyperparameters of the Deep Learning Models

Models	Batch Size	Loss Functions	Learning Rate
Transformer UNet	4	Dice Loss	1×10^{-4}
Super Vision UNet	8	Dice Loss	1×10^{-4}
UNet	8	Dice Loss	1×10^{-3}

An analysis of the hyperparameter settings (Table 3) shows that models trained using Dice Loss outperformed those trained with alternative loss functions such as Binary Cross Entropy (BCE). This suggests that Dice Loss provides a more effective learning process for medical segmentation tasks involving class imbalance, such as distinguishing between tumor and healthy tissue in MRI scans, thus enhancing segmentation performance.

Figure 3 displays example segmentation results from selected image slices. A visual examination reveals that both Transformer UNet and Super Vision UNet consistently generate segmentation masks that are closely aligned with the ground truth, particularly in terms of boundary fidelity and completeness of tumor regions. Notably, these models were able to

capture finer details at the tumor margins and reduce under- and over-segmentation issues. Super Vision UNet, in particular, appears to better delineate subtle tumor edges, which may contribute to its superior Dice Coeff performance. On the other hand, the UNet model occasionally exhibits under-segmentation (missing parts of the tumor) or boundary inaccuracies, especially in more complex or infiltrative cases, as seen in the third and eighth columns of Figure 3.

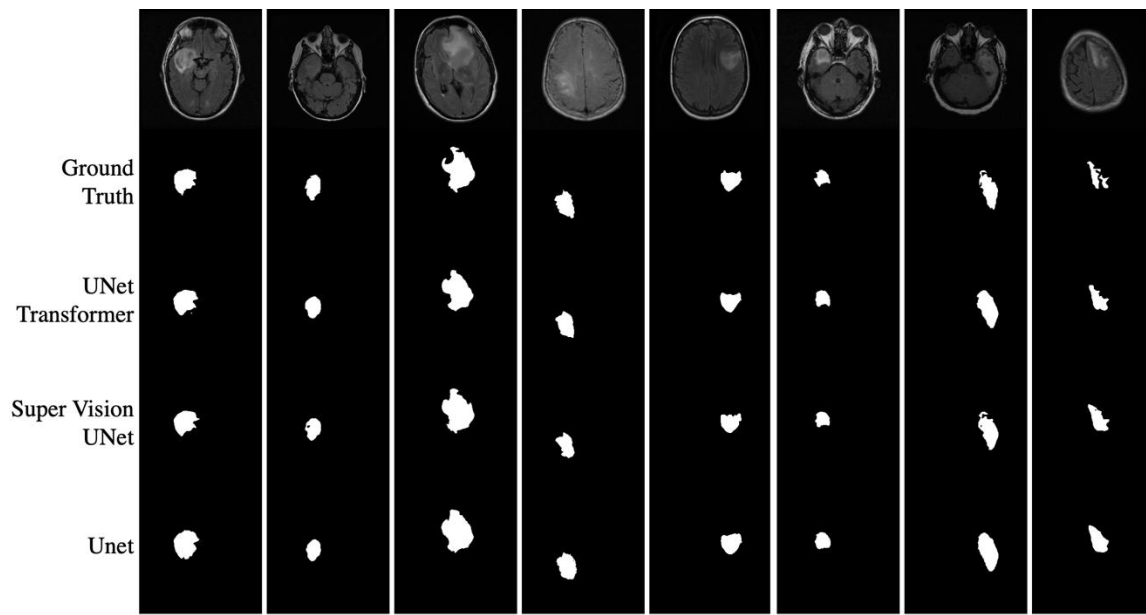


Figure 3. Sample prediction results from the models

Previous studies in the literature (e.g., Naser & Deen, 2020; Lefkovits et al., 2022) have also demonstrated the effectiveness of deep learning models in brain tumor segmentation, while emphasizing that architectural modifications can further enhance accuracy. The findings from this study reinforce the idea that modern variants of UNet, such as Transformer UNet and Super Vision UNet, have significant potential for more precise boundary delineation, particularly in LGGs, which often exhibit infiltrative and heterogeneous characteristics. Additionally, the use of Dice Loss, which is more sensitive to class imbalance, appears to be a critical factor in achieving higher model performance. This loss function's alignment with the structure of medical imaging data helps the models better distinguish between tumor and non-tumor regions.

In summary, both the quantitative results (Tables 2 and 3) and qualitative visual assessments (Figure 3) indicate that Transformer UNet and Super Vision UNet outperform the traditional UNet in LGG segmentation. The comparable performance of these two models suggests that both are strong candidates for deep learning-based medical image segmentation tasks.

CONCLUSION

In this study, three different deep learning models—Transformer UNet, Super Vision UNet, and the conventional UNet—were evaluated for the task of low-grade glioma (LGG) segmentation in brain MRI images. The results indicate that enhanced UNet-based approaches and Transformer-based architectures achieved higher Tversky Index, Dice Coefficient, and IoU scores compared to the traditional UNet, thus delivering more accurate segmentation performance. Furthermore, the segmentation masks produced by these models closely reflect the actual tumor boundaries, highlighting the strong potential of deep learning models in medical image analysis.

Accurate and efficient segmentation is especially critical in the case of LGGs, which, although classified as low-grade, possess an infiltrative nature. Reliable segmentation can significantly support clinical decision-making processes. The automatic segmentation capabilities offered by these models may help reduce the workload of radiologists and neurosurgeons while minimizing subjective errors.

Future studies may focus on further improving these models by training them on larger and more diverse datasets and evaluating their effectiveness across different tumor grades. Additionally, integrating multimodal data, such as genomic and clinical information, into deep learning frameworks could enhance the precision and utility of such systems, offering more comprehensive support in the diagnosis and management of gliomas.

REFERENCES

- BabaAhmadi, A. & FallahPour, Z. (2023). Efficient Deep Learning Algorithms for Lower Grade Gliomas Cancer MRI Image Segmentation: A Case Stud. *AUT Journal of Mathematics and Computing*, (Online First). <https://doi.org/10.22060/ajmc.2023.22562.1172>
- Bentaher, N., Lafraxo, S., Kabbadj, Y., Ben Salah, M., El Ansari, M. & Wakrim, S. (2025). R2A-UNET: double attention mechanisms with residual blocks for enhanced MRI image segmentation. *Multimedia Tools and Applications*, 1-31.
- Buda, M., Saha, A. & Mazurowski, M. A. (2019). Association of genomic subtypes of lower-grade gliomas with shape features automatically extracted by a deep learning algorithm. *Computers in Biology and Medicine*, 109, 218–225. <https://doi.org/10.1016/j.compbiomed.2019.05.002>
- Buda, M. (2019). *LGG MRI Segmentation* [Data set]. Kaggle. <https://kaggle.com/datasets/mateuszbudalgg-mri-segmentation>
- Dattangire, R., Biradar, D. & Joon, A. (2024). AI-Enhanced U-Net for Accurate Low-Grade Glioma Segmentation in Brain MRI: Transforming Healthcare Imaging. *2024 Third International Conference on Electrical, Electronics, Information and Communication Technologies (ICEEICT)*, 1–6. Trichirappalli, India: IEEE. <https://doi.org/10.1109/ICEEICT61591.2024.10718440>
- Ghadimi, D. J., Vahdani, A. M., Karimi, H., Ebrahimi, P., Fathi, M., Moodi, F., ... Saligheh Rad, H. (2025). Deep Learning-Based Techniques in Glioma Brain Tumor Segmentation Using Multi-Parametric MRI: A Review

-
- on Clinical Applications and Future Outlooks. *Journal of Magnetic Resonance Imaging*, 61(3), 1094–1109. <https://doi.org/10.1002/jmri.29543>
- Jaccard, P. (1912). The Distribution Of The Flora In The Alpine Zone. *New Phytologist*, 11(2), 37–50. <https://doi.org/10.1111/j.1469-8137.1912.tb05611.x>
- Le'Clerc Arrastia, J., Heilenkötter, N., Otero Bager, D., Hauberg-Lotte, L., Boskamp, T., Hetzer, S., ... Maass, P. (2021). Deeply Supervised UNet for Semantic Segmentation to Assist Dermatopathological Assessment of Basal Cell Carcinoma. *Journal of Imaging*, 7(4), 71. <https://doi.org/10.3390/jimaging7040071>
- Lefkovits, S., Lefkovits, L. & Szilágyi, L. (2022). HGG and LGG Brain Tumor Segmentation in Multi-Modal MRI Using Pretrained Convolutional Neural Networks of Amazon Sagemaker. *Applied Sciences*, 12(7), 3620. <https://doi.org/10.3390/app12073620>
- Louis, D. N., Perry, A., Reifenberger, G., Von Deimling, A., Figarella-Branger, D., Cavenee, W. K., ... Ellison, D. W. (2016). The 2016 World Health Organization Classification of Tumors of the Central Nervous System: A summary. *Acta Neuropathologica*, 131(6), 803–820. <https://doi.org/10.1007/s00401-016-1545-1>
- Milletari, F., Navab, N. & Ahmadi, S.-A. (2016). V-Net: Fully Convolutional Neural Networks for Volumetric Medical Image Segmentation. *2016 Fourth International Conference on 3D Vision (3DV)*, 565–571. Stanford, CA, USA: IEEE. <https://doi.org/10.1109/3DV.2016.79>
- Naser, M. A. & Deen, M. J. (2020). Brain tumor segmentation and grading of lower-grade glioma using deep learning in MRI images. *Computers in Biology and Medicine*, 121, 103758. <https://doi.org/10.1016/j.compbiomed.2020.103758>
- Ostrom, Q. T., Bauchet, L., Davis, F. G., Deltour, I., Fisher, J. L., Langer, C. E., ... Barnholtz-Sloan, J. S. (2014). The epidemiology of glioma in adults: A “state of the science” review. *Neuro-Oncology*, 16(7), 896–913. <https://doi.org/10.1093/neuonc/nou087>
- Pedano, N., Flanders, A. E., Scarpace, L., Mikkelsen, T., Eschbacher, J. M., Hermes, B., ... Ostrom, Q. (2016). *The Cancer Genome Atlas Low Grade Glioma Collection (TCGA-LGG) (Version 3) [Data set]*. The Cancer Imaging Archive. <https://doi.org/10.7937/K9/TCIA.2016.L4LTD3TK>
- Petit, O., Thome, N., Rambour, C., Themyr, L., Collins, T. & Soler, L. (2021). U-Net Transformer: Self and Cross Attention for Medical Image Segmentation. In C. Lian, X. Cao, I. Rekik, X. Xu, & P. Yan (Eds.), *Machine Learning in Medical Imaging* (pp. 267–276). Cham: Springer International Publishing. https://doi.org/10.1007/978-3-030-87589-3_28
- Ronneberger, O., Fischer, P. & Brox, T. (2015). U-Net: Convolutional Networks for Biomedical Image Segmentation. In N. Navab, J. Hornegger, W. M. Wells, & A. F. Frangi (Eds.), *Medical Image Computing and Computer-Assisted Intervention – MICCAI 2015* (pp. 234–241). Cham: Springer International Publishing. https://doi.org/10.1007/978-3-319-24574-4_28
- Sanai, N. & Berger, M. S. (2008). Glioma Extent Of Resection and Its Impact on Patient Outcome. *Neurosurgery*, 62(4), 753–766. <https://doi.org/10.1227/01.neu.0000318159.21731.cf>
- Shomirov, A., Zhang, J. & Billah, M. M. (2022). Brain Tumor Segmentation of HGG and LGG MRI Images Using WFL-Based 3D U-Net. *Journal of Biomedical Science and Engineering*, 15(10), 241–260. <https://doi.org/10.4236/jbise.2022.1510022>
- Tversky, A. (1977). Features of similarity. *Psychological Review*, 84(4), 327–352. <https://doi.org/10.1037/0033-295X.84.4.327>
- Van Dijken, B. R. J., Van Laar, P. J., Holtman, G. A. & Van Der Hoorn, A. (2017). Diagnostic accuracy of magnetic resonance imaging techniques for treatment response evaluation in patients with high-grade glioma, a systematic review and meta-analysis. *European Radiology*, 27(10), 4129–4144. <https://doi.org/10.1007/s00330-017-4789-9>

Verma, A., Shivhare, S. N., Singh, S. P., Kumar, N. & Nayyar, A. (2024). Comprehensive Review on MRI-Based Brain Tumor Segmentation: A Comparative Study from 2017 Onwards. *Archives of Computational Methods in Engineering*, 31(8), 4805–4851. <https://doi.org/10.1007/s11831-024-10128-0>

Wan, B., Hu, B., Zhao, M., Li, K. & Ye, X. (2023). Deep learning-based magnetic resonance image segmentation technique for application to glioma. *Frontiers in Medicine*, 10, 1172767. <https://doi.org/10.3389/fmed.2023.1172767>